



Magma Chamber Rejuvenation: Insights from Numerical Models

C.P. Montagna, P. Papale, A. Longo and M. Bagagli

Abstract

Most volcanic systems on Earth are characterized by chemically different magmas that can be found in the erupted products throughout their history. The reasons are multiple, including variations in the mantle source and/or crustal assimilation, as well as shallower processes such as fractional crystallization or mixing and mingling. Magma chamber rejuvenation indicates the processes that happen whenever a magma intrudes from the mantle to shallower depths and encounters an already established storage zone (i.e. a magma chamber or reservoir). Magmas rising from depth are typically characterized by higher temperatures, larger volatile contents and more primitive, mantle-like compositions than those residing in the shallow crust. The interaction with magmas that have already resided at shallower depths for a while (years to thousands of years) varies the physical and chemical properties of both the involved magmatic end-members. Typically, volatile-rich magmas coming from depth are lighter than degassed shallow magma; therefore, a gravitational instability sets in as the two come into contact, which generates convection and thus intense mingling and mixing among the two. These dynamic interactions cause variations in the physical and chemical properties of the magmas themselves, as well as in the stress conditions both inside the reservoir and in the host rock. The volcanic system as a whole enters an unrest scenario, that can evolve to eruption or not depending on the specific conditions. Numerical simulations of the dynamics within magmatic systems can shed light on the features of magma chamber rejuvenation, providing the time

C.P. Montagna (✉) · P. Papale · A. Longo ·
M. Bagagli
Istituto Nazionale di Geofisica e Vulcanologia, via
U. della Faggiola 32, Pisa, Italy
e-mail: chiara.montagna@ingv.it

Present Address:

M. Bagagli
D-ERDW, ETH-Zuerich, Zürich, Switzerland

Adv in Volcanology (2019) 111–122

DOI [10.1007/11157_2017_21](https://doi.org/10.1007/11157_2017_21)

© The Author(s) 2017

Published Online: 17 August 2017

scales of mixing processes and possibly of the evolution towards eruption. Coupling with models for the visco-elastic response of the host rock allows the identification of the onset of recharge processes from the analysis of geophysical signals observed at the surface.

Keywords

Magma chamber · Magma dynamics · Magma mixing

1 Extended English/Spanish abstract

Most volcanic systems on Earth are characterized by chemically different magmas that can be found in the erupted products throughout their history, either in synchronous eruptive episodes, or in different epochs of volcanic activity. This chemical heterogeneity can have multiple reasons, and it originates from deep in the mantle, due to variations in the source and/or crustal assimilation during ascent, to shallower crustal regions, where processes such as fractional crystallization or mixing and mingling take place. Magma chamber rejuvenation comprises some of the aforementioned processes at shallow level. Whenever a magma intrudes from the mantle to shallower depths and encounters an already established storage zone (a magma chamber or reservoir), the magma already emplaced gets rejuvenated by the incoming more primitive magma. Magmas rising from the deep regions of a volcano feeding system are typically characterized by higher temperatures, larger volatile contents and more primitive, mantle-like compositions. On the other hand, magmas that have resided at shallower depths for a while (years to thousands of years) have evolved by fractional crystallization, thus they have changed their composition towards a more felsic one, and have lost most of their gaseous phase, that can escape towards the surface. The interaction between primitive and evolved magmas varies the physical and chemical properties of both the end-members involved. Typically, volatile-rich magmas coming from depth are lighter than degassed shallow magma, albeit

having a higher liquid density: they are characterized by a much larger gas content. The light magma tends to rise inside the denser reservoir; a gravitational instability sets in as the two magmatic mixtures come into contact, and generates convection inside the reservoir. As a consequence, intense mingling and mixing are generated among the two end-members. These dynamic interactions cause variations in the physical and chemical properties of the magmas themselves, that lose their identity as initial end-members and become a more homogeneous mixture. The volcanic system as a whole enters an unrest scenario, that can evolve to eruption or not depending on the specific conditions. Numerical simulations of a magmatic system representing magma injection into a shallow reservoir show that mixing is very intense at the time of contact, and can be efficient on time scales of hours to day in homogenizing the system. Depending on the geometry of the volcano feeding system, and even more on the volatile content of the incoming and resident magmas, the process can be suppressed or enhanced. Sills favour mixing, while more vertically elongated, dike-like reservoirs slow the dynamical interactions. As the presence of a gaseous phase is the engine of the gravitational instability that triggers the dynamics, a higher volatile content, which translates into a higher gas content, in the deep regions of the feeding system strongly accelerates the rejuvenation process. As mixing patterns are found almost ubiquitously in products from volcanoes around the world, comparison of the observed features to the model predictions can provide insights on the features of magma chamber rejuvenation, including the time

scales over which mixing processes are efficient and possibly the timings for the evolution towards an eruption or not. Coupling to models that describe the visco-elastic response of the host rock to stress variations within the magmatic system provides hints as to how to identify recharge processes at depth from the analysis of geophysical signals observed at the surface. Characteristic features of ground deformation associated to convection and mixing is the appearance of oscillation of extremely long period, on the order of hours (Ultra-Long-Period, ULP), that can be detected by instruments such as continuous tiltmeters and dilatometers. Their records can identify the onset of the interaction among different magmas, thus provide time scales for unrest duration and evolution.

2 Introduction

Magmas evolve in many ways during their residence time within the crust, determining whether they are going to be erupted or not. Magma chamber rejuvenation takes place whenever a magma intruding from the mantle to shallower depths encounters an already established storage zone (i.e. a magma chamber or reservoir). It can involve many different processes such as reheating and melting of the residing magmas, fractional crystallization due to changes in the pressure and temperature conditions, mingling and mixing among the different components; typically, it takes place at shallow crustal depths. Magmas rising from depth are often characterized by higher temperatures, larger volatile contents and more primitive, mantle-like compositions with respect to those that have been residing at shallower levels for a while (months, years to thousands of years). This general scenario can have a variety of declinations, depending on the specific setting and physico-chemical characteristics of the magmatic mixtures involved. The shallow magma can be highly crystalline, a mush, that can be rejuvenated by the heat from the incoming component (Bachmann and Bergantz 2003, 2008; Girard and Stix 2009; Bain et al. 2013; Till et al. 2015); or, at the other end, it can still be hot and

more fluidal, especially if injection episodes are frequent (Voight et al. 2010), giving rise to mixing and mingling phenomena (Montagna et al. 2015). The interaction among the deep and shallow components changes the physical and chemical properties of both the involved magmatic end-members, triggering an unrest phase that can evolve to eruption or not depending on the specific conditions. Evidence of chamber rejuvenation both in igneous and in intrusive rocks, manifested mostly by mingling and mixing patterns, is almost ubiquitous at volcanic systems worldwide, and it is often invoked as eruption trigger.

Magma movement at depth implies mass re-distribution, pressure changes, and pressure transients which translate into variations in the gravity field, shape and slope of the volcano flanks, and seismic signals registered at the surface. Understanding the complex relationships between quantities measured by volcano monitoring networks and shallow magma processes is a crucial step for the comprehension of volcanic processes and in evaluating more realistic hazard forecast. The ability to detect the onset of magma recharge at depth is fundamental as it can provide hints to unrest duration and evolution, and possibly eruption timings.

In this work we describe a forward-modeling approach to describe magma chamber dynamics, specifically for what concerns rejuvenation episodes, and link it to the geophysical observables that are expected as a consequence. This provides a framework for the consistent interpretation of geological and geophysical records of unrest periods at active volcanoes. This methodology allows for identification of rejuvenation episodes in ground deformation records, and possibly discrimination between those episodes that lead to eruption or not.

3 Numerical Simulations of Magma Chamber Rejuvenation

3.1 Magmatic System

We refer as an archetypal case to the Phlegraean Fields magmatic system, where seismic imaging and attenuation tomographies have identified a

huge (probably around 10 km wide) magma reservoir at a depth of around 8 km (Zollo et al. 2008; De Siena et al. 2010), while a variety of geophysical and geochemical evidence suggests that smaller (probably less than 1 km³), shallower batches of magma have been forming throughout the caldera history at virtually any depth smaller than 9 km (Arienzo et al. 2010; Di Renzo et al. 2011). These shallow magma bodies have been identified as actively involved in past eruptions, which at least in some cases shortly followed the arrival of volatile-rich, less differentiated magmas from the deep feeding system (Arienzo et al. 2009; Fourmentraux et al. 2012). Chemical compositions of erupted magmas range from shoshonitic to trachytic to phonolitic; geochemical analyses on melt inclusions suggest a variety of processes contributing to this variability, such as recharge from depth, intra-chamber mixing, syn-eruptive mingling (Arienzo et al. 2010; Fourmentraux et al. 2012). The same analyses

show that deep magmas are typically rich in gas, especially CO₂ (Mangiaccapra et al. 2008), while shallow magmas are unusually crystal-poor, down to less than 3 wt% (Arienzo et al. 2009). To study the magmatic dynamics occurring as a consequence of a recharge event, we simplify the magmatic system retaining its most peculiar features. We model the injection of CO₂-rich shoshonitic magma coming from a deep reservoir into a shallower, much smaller chamber, containing more evolved and partially degassed phonolitic magma (see Table 1 for compositions). The two chambers are connected by a dyke. This idealized layout captures several first-order characteristics of prototype magmatic systems, including a composite structure, vertical extension, and heterogeneous composition, and it approximates systems composed by long-lived, interconnected multiple reservoirs believed to exist at many active volcanoes (Elders et al. 2011).

Table 1 Composition of the phonolite and shoshonite magma types employed in the simulations

Composition	SiO ₂ (wt%)	TiO ₂ (wt%)	Al ₂ O ₃ (wt%)	Fe ₂ O ₃ (wt%)	FeO (wt%)	MnO (wt%)	MgO (wt%)	CaO (wt%)	Na ₂ O (wt%)	K ₂ O (wt%)
Phonolite	53.5	0.6	19.8	1.6	3.2	0.1	1.8	6.8	4.7	7.9
Shoshonite	52.5	0.9	17.6	1.9	5.7	0.1	3.6	7.9	3.4	4.3

Fig. 1 Initial conditions for the numerical simulations of the magmatic system. On the *left*, the whole domain is shown, indicating the two magmatic end-members. On the *right*, the *upper* portion of the domain shows the three different geometries explored

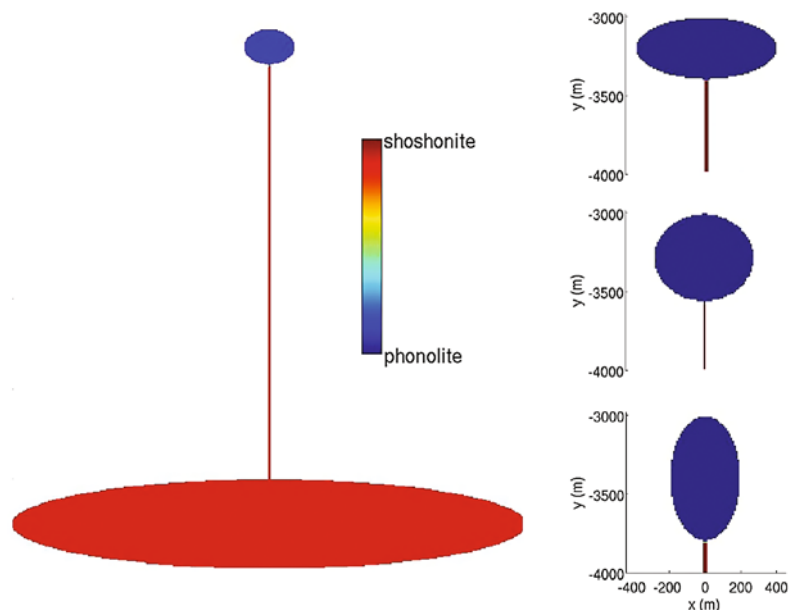


Figure 1 shows the system domain for the numerical simulations. We assume one of the horizontal dimensions of the magmatic system to be much larger than the other, so that our domain is two-dimensional. The deep chamber is elliptical, 1 km thick and 8 km wide; its top is at 8 km depth. The geometry of the shallow chamber has been varied as shown in Fig. 1, keeping its surface area fixed. In the elliptical cases, the semi-axes measure 400 and 800 m, respectively, while the circular chamber has a radius of 283 m.

The initial conditions of the system are also shown in Fig. 1. The shallow chamber hosts a differentiated, volatile-poor phonolitic magma. Its volatile content has been varied from 0.3 wt% CO₂ and 2.5 wt% H₂O to 0.1 wt% CO₂ and 1 wt% H₂O. In the feeding dyke and deep reservoir is a less evolved, basaltic shoshonite, containing 1 wt% CO₂ and 2 wt% H₂O. Such a low water content in the phonolitic end-member derives from melt inclusion data from Phlegrean Fields (Arienzo et al. 2010). Typically, more evolved magmas are expected to have a relatively larger water content (Signorelli et al. 2001; Cannatelli et al. 2007; Pappalardo et al. 2007; Mollo et al. 2015), resulting possibly in smaller density contrasts at the interface among the two magmas thus less efficient mixing dynamics.

Volatiles partitioning between gaseous and liquid phases is computed following Papale et al. (2006) as a function of composition and pressure. Pressure at time 0 consists of a depth-dependent

turn depends on pressure, thus on the depth at which the interface is placed, which is different for each geometry of the shallow chamber (Fig. 1). Temperature differences between interacting magmas are often negligible (Sparks et al. 1977), particularly at Phlegrean Fields (Mangiaccapra et al. 2008; Arienzo et al. 2010), thus the system is assumed isothermal. As a result, there is no need to speculate on the thermal status of the surrounding rock, thus reducing model uncertainties. Moreover, heat transfer effects are expected to play a minor role on the short simulated time scales (hours; Di Renzo et al. 2011).

3.2 Magma Dynamics

Interaction among the two magmas develops as a consequence of the initial gravitational instability at the interface. We solve numerically the two-dimensional space-time evolution of the system, consisting of a mixture of two different magmatic components, each of them including a liquid (silicate melt and dissolved volatiles) and a gaseous (exsolved volatiles) fractions. The equations of motion for the mixture express conservation of mass for each component $k = 1, 2$, and momentum for the whole mixture (Longo et al. 2012a):

$$\frac{\partial(\rho y_k)}{\partial t} + \nabla \cdot (\rho \mathbf{u} y_k) = -\nabla \cdot (\rho D_k \nabla y_k), \quad \sum_k y_k = 1 \quad (1)$$

$$\frac{\partial(\rho \mathbf{u})}{\partial t} + \mathbf{u} \cdot \nabla (\rho \mathbf{u}) = -\nabla p + \nabla \cdot \left\{ \mu \left[\nabla \mathbf{u} + (\nabla \mathbf{u})^T - \frac{2}{3} \nabla \cdot \mathbf{u} \right] \right\} + \rho \mathbf{g}. \quad (2)$$

magmastic contribution superimposed to the host rock confining pressure. The interface between the two magmas, at the inlet of the shallow chamber, is gravitationally unstable, the lower magma being less dense due to its higher gas content. The dynamics is solely driven by buoyancy, without any external forcing.

The density contrast at the interface varies for each simulated scenario, as it depends on both volatiles content and their partitioning between liquid and gaseous phases; volatiles exsolution in

In the above, t is time; ρ is mixture density, y_k is mass fraction of component k , \mathbf{u} is fluid velocity, D_k is the k -th coefficient of mass diffusion, p is pressure, μ is viscosity and \mathbf{g} is gravity acceleration.

The magmatic mixture is considered ideal. Its density is evaluated as weighted sum of the components' densities; for each component, density is calculated using a non-ideal equation of state for the liquid phase, real gas properties and ideal mixture laws for multiphase fluids.

Mixture viscosity is computed through standard rules of mixing for one phase mixtures and with a semi-empirical relation in order to account for the effect of non-deformable gas bubbles. Liquid viscosity is modeled as in Giordano et al. (2008), and it depends on liquid composition and dissolved water content. The assumption of Newtonian rheology is justified by the very low strain rates and the crystal-free nature of the magmas. The generalized Fick's law is used to describe mass diffusion. Volatile partitioning between gaseous and liquid phases is evaluated at every point in the space-time domain as function of mixture composition and pressure as in Papale et al. (2006). All the physical properties of the two magmas are evaluated at every point in the space-time domain depending on the local conditions of pressure, velocity and mass fractions, which are the unknowns in Eqs. (1) and (2). The equations are solved numerically using GALES, a finite element C++ code specifically designed for volcanic fluid dynamics (Longo et al. 2012a).

The evolution in space and time of the system is complex and presents a number of interesting features. Figure 2 summarizes the results regarding initial magma dynamics, showing the evolution of

composition in time in the shallow chamber for the five different simulation scenarios.

The initial inverse density contrast at the contact interface between the two magmas gives rise to convective mass transfer from the deeper parts of the system to shallower depths and vice versa. The unstable density contrast is solely due to the different volatile content of the two mixtures: the shoshonitic melt has a higher density than the phonolitic. The role played by volatiles is crucial, and it is exsolved gases that ultimately determine the buoyant dynamics. A Rayleigh-Taylor instability develops, which acts to bring the system to gravitational equilibrium by overturning it. The instability develops starting from the perturbed interface, with a first plume of light material that rises into the chamber. Depending on the initial density contrast as well as on the geometry of the shallow chamber, the initial plume starts developing at different times. The dynamics is strongly enhanced by higher density contrasts; geometry also plays an important role when density contrasts are similar, with horizontally elongated, sill-like chambers favouring convection with respect to more dyke-like setups (see also Fig. 2).

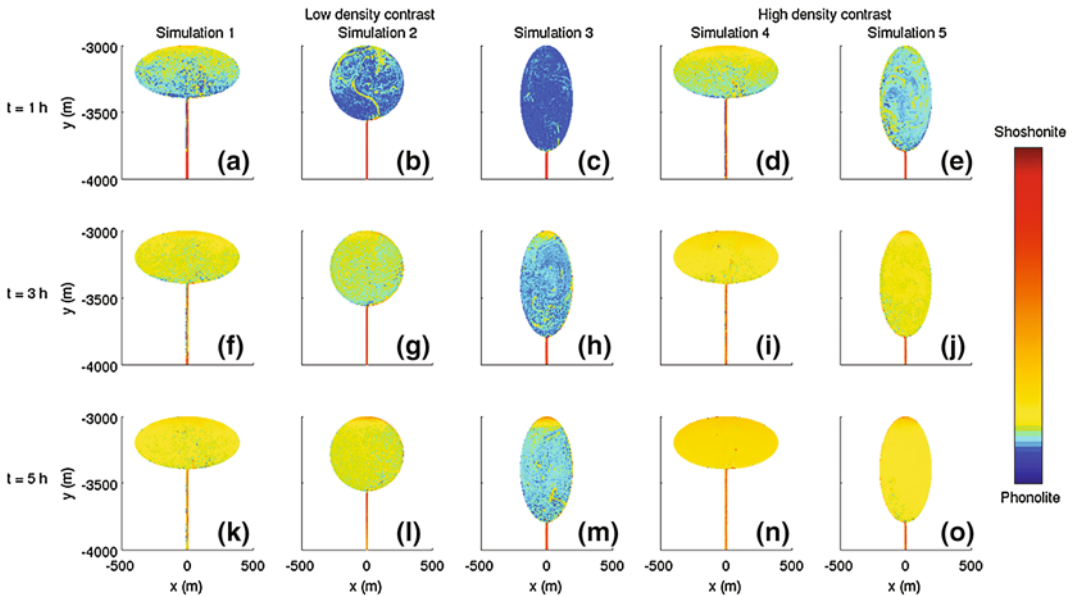


Fig. 2 Snapshots of variation of composition with time in the shallower parts of the system for the different simulations. *Columns* correspond to different simulations; *rows* correspond to different times

Plumes of light magma coming from depth keep entering the shallow reservoir as discrete filaments, following irregular trajectories and showing typical convective patterns. The lighter material tends to rise into the chamber, thereby decreasing more and more its density as volatiles exsolve in lower-pressure environments; on the other hand, the denser magmatic mixture initially residing in the chamber sinks into the feeder dyke, increasing its density by the reverse process of volatile dissolution at higher pressures. The plumes thus progressively increase their buoyancy, enhancing their expansion and acceleration. During the rise, vortices form at the head of the plumes and subsequent plumes interact among themselves, further favouring mixing. The dynamics creates complicated patterns that maximize the interaction among the two different magmatic mixtures (Petrelli et al. 2011). Mingling is evident for all simulated conditions both within the chamber itself and even more in the feeding dyke (Fig. 2), and it is strongly intensified by the chaotic patterns that form as a consequence of deep magma injection.

Independently from system geometry or density contrast at the interface, mingling is very efficient in the feeding dyke, more than inside the upper chamber. Figure 2 shows that since the very beginning of the simulations, the magma entering the chamber is already a mixture of the

two initial end-members, and not the pure shoshonitic composition.

As the dynamics proceeds, faster for higher density contrasts and sill-like setups, the gas-rich mixture tends to accumulate at the top of the chamber, thereby originating a stable density stratification that has indeed been testified at various magmatic systems (Arienzo et al. 2009). The stratification is more prominent in vertically elongated, dyke-like reservoirs (Fig. 2). The density profile along the vertical direction, evaluated averaging along horizontal planes (Fig. 3), illustrates that a quasi-stable profile is reached after some hours of simulated time.

As time proceeds, convection slows down due to smaller buoyancy of the incoming already mixed component, and the instability proceeds in time asymptotically: the more the two end-members have mingled, the less intense is convection.

The evolution of pressure in the system is highly heterogeneous in space and time. Alternating phases dominated by buoyancy and sinking at chamber inlet result in pressure fluctuations with periods of hundreds of seconds and amplitudes decreasing with time (Fig. 4). Typically pressure variations are smaller than 1 MPa; under these conditions, it is unlikely that rejuvenation can trigger eruption, as the stresses needed to create a pathway to the surface in the host rock are typically larger than that (Gudmundsson 2006).

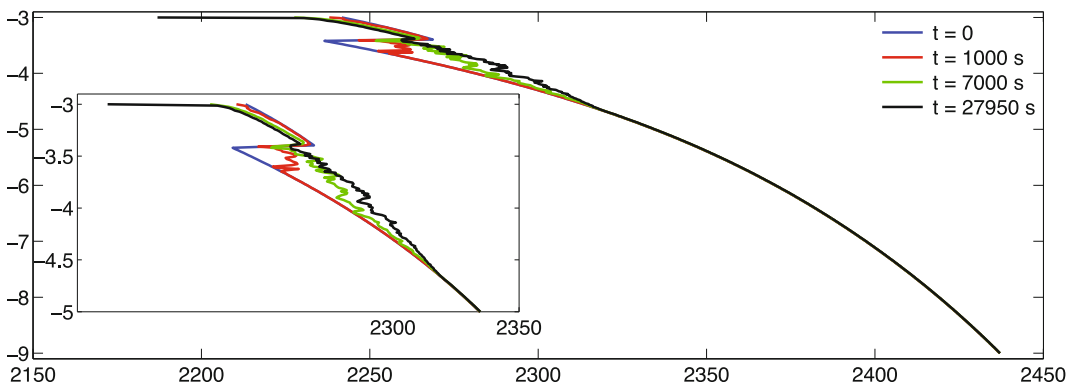


Fig. 3 Total mixture density averaged over horizontal planes as function of depth for simulation 1, at different times. The inset shows the upper 5 km of the domain; the

black line represents the quasi-equilibrium density profile at the end of the simulation

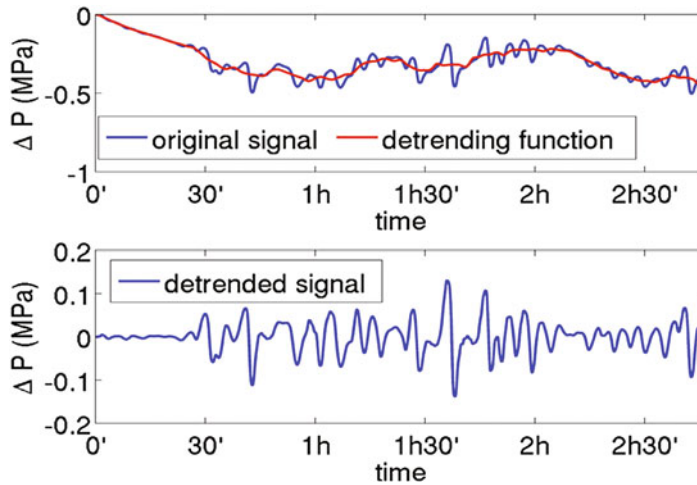


Fig. 4 Pressure variations as a function of time at a point on the boundary of the upper chamber, for simulation #1. The *upper* diagram shows the difference between the local

pressure at current time and at time zero, while the *bottom* diagram shows the same quantity after subtraction of a detrrending function (*red curve* in the *upper* diagram)

3.3 Ground Deformation

Determining the time–space-dependent ground displacement requires modeling the magma–rocks boundary conditions and the mechanical response of rocks, the latter depending on heterogeneous rock properties, presence and distribution of faults, interfaces, fluids, and volcano topography (e.g., O’Brien and Bean 2004). A first-order analysis performed here assumes magma–rock one-way coupling and adopts the Green’s functions formulation for a homogeneous, infinite medium (Aki and Richards 2002).

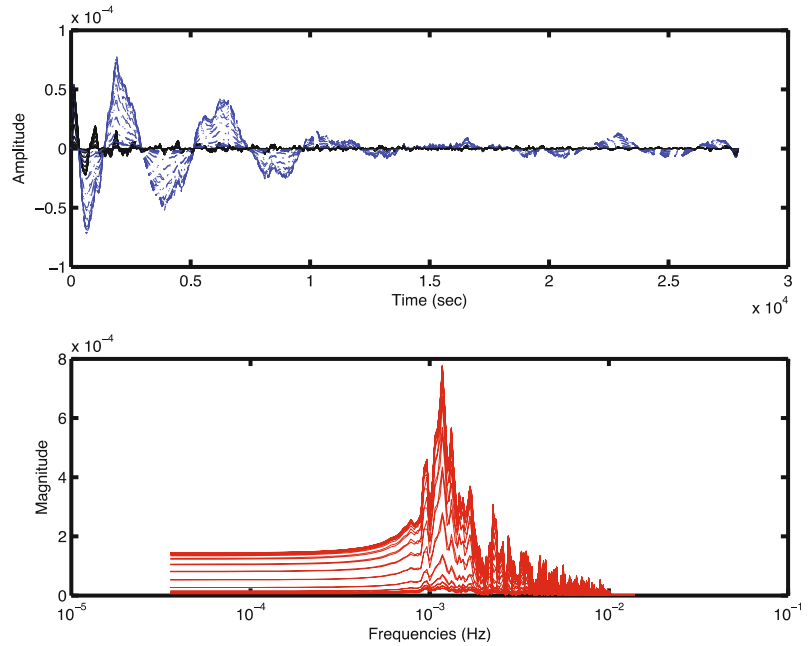
We consider as point sources the fluid dynamics computational grid nodes located at the reservoir walls. As source time functions, we use the respective temporal evolutions of magmatic forces computed from pressures and stresses provided at those nodes by the numerical simulations of magma convection and mixing dynamics. Ground displacement at a series of virtual receivers is finally obtained by integrat-

ing, over all sources, the Green’s functions associated with individual sources.

Continuity of pressure and stress is taken as the boundary condition along the non moving magma–rock interface. Physical properties of rocks are homogeneous averages that describe the volcanic edifices within the range of considered depths (<10 km, $v_P = 3000$ m/s; $v_P/v_S = 1/\sqrt{3}$, $\rho = 2500$ kg/m³).

Propagation of pressure disturbances in the host rock medium reveals that the computed pressure oscillations, originated by the ingress of buoyant magma in the magma chamber, translate into Ultra Long Period ground displacement dynamics with amplitudes of millimeter to micrometer order (Fig. 5; Longo et al. 2012b). ULP ground movements like those predicted by the present modeling could not be detected by classical broadband seismometers (although more recent seismometers extend their working range up to 100–200 s periods), while they are visible in the records from other instruments, especially

Fig. 5 Synthetic seismic signal (*blue* detrended as to represent an instrumental record, *black* filtered [0.001,0.01] Hz) and corresponding frequency spectrum for the vertical component at all synthetic stations. Example from simulation #1



borehole dilatometers characterized by high signal-to-noise ratio (Sacks et al. 1971).

4 Discussion and Conclusions

The arrival of fresh magma into an already emplaced reservoir and the consequent internal dynamics have often been invoked as possible eruption triggers, especially at Phlegraean Fields (Arienzo et al. 2010); on the other hand, footprints of magma chamber rejuvenation are often found in intrusive granites as well, testifying that it does not necessarily lead to eruption. Magma chamber rejuvenation can thus be regarded as a prototypical volcanic unrest process, that can lead to eruption or not depending on the specific system conditions (e.g. host rock compliance, volume and volatile content of injected magma).

The time scales for rejuvenation processes to be effective in magmatic reservoirs are relatively short, on the order of hours. This is consistent with what has been observed from the analyses of erupted products (Fourmentraux et al. 2012) as well as from experiments on diffusive fractionation (Perugini et al. 2010), and opens a completely new perspective in terms of unrest

duration: indications of mixing in erupted products suggest that recharge events can happen within a very short time frame from eruption, otherwise the evidence would be wiped out by the efficient mixing process (Montagna et al. 2015).

In terms of geophysical observables, convective mingling dynamics in magmatic reservoirs is associated with ultra-long-period seismic signals, characterized by frequencies in the range $10^{-2} - 10^{-4}$ Hz (Longo et al. 2012b).

The results obtained by our modeling specifically refer to the Phlegraean system. They can be extended to many other volcanoes where evidence of rejuvenation has been observed in similar magmatic settings, characterized by relatively primitive magmas that are not very different in composition and temperature, such as e.g. Mount Etna (Viccaro et al. 2006) or Stromboli (La Felice et al. 2011). For more evolved magmas, reservoirs can be dominated by crystal-rich regions (Marsh 1981; Koyaguchi and Kaneko 1999; Bachmann and Bergantz 2004; Hildreth 2004; Huber et al. 2009; Cooper and Kent 2014), and they are often at a lower temperature. The approach described above must be applied with caution in such cases, as the dynamics of the incoming primitive magma is

more likely to be described as flow through a porous medium (mush) than as fluid mingling and mixing. Nonetheless, there is some evidence for crystal-poor silicic magma reservoirs to be reactivated as well (Bachmann et al. 2002; Deering et al. 2011; Huber et al. 2012; Sliwinski et al. 2015; Wolff et al. 2015).

Given the short time scales over which the dynamical processes described here can be effective and lead to eruption, it would be beneficial to be able to routinely detect the signals described above for eruption forecasting and mitigation actions. This is especially true for long-dormant volcanoes such as Phlegraean Fields, one of the highest-risk volcanic areas in the world given the large population living within the caldera borders (Arienzo et al. 2010), for which there is still no widely accepted means of discriminating the precursors of an impending eruption (Druitt et al. 2012).

Acknowledgements This work has received funds from the European Union's Seventh Programme for research, technological development and demonstration under grant agreements No. 282769 VUELCO and No. 308665 MED-SUV. The manuscript has largely benefited from reviews by Fabio Arzilli and Olivier Bachmann.

Glossary

Magma chamber A storage volume for magma in the crust. Typically, during their rise from the mantle magmas accumulate in regions where there are geological discontinuities.

Rejuvenation The process by which magmas coming from depth modify chemical and physical properties of more evolved magmas already emplaced at shallower levels.

Primitive magma A magmatic melt that has composition similar to that of the mantle (smaller silica content).

Evolved magma A magmatic melt that has undergone processes within the crust that modified its chemical properties, such as fractional crystallization and crustal assimilation.

Its composition is characterized by higher silica content.

Convection Exchange of mass and energy by means of cell patterns.

Green's functions Source to receiver transfer function; in this context through the volcanic rock medium.

Index

Volcanic unrest
Magma chamber dynamics
Magma mingling: magma mixing
Eruption precursors
Volcanic unrest duration
Magma evolution
Ground deformation
Ultra-Long-Period seismicity
Volcano seismicity

References

- Aki K, Richards PG (2002) Quantitative seismology. University Science, Sausalito
- Arienzo I, Civetta L, Heumann A, Woerner G, Orsi G (2009) Isotopic evidence for open system processes within the Campanian Ignimbrite (Campi Flegrei—Italy) magma chamber. *Bull Volcanol* 71(3):285–300
- Arienzo I, Moretti R, Civetta L, Orsi G, Papale P (2010) The feeding system of Agnano—Monte Spina eruption (Campi Flegrei, Italy): Dragging the past into present activity and future scenarios. *Chem Geol* 270 (1–4):135–147
- Bachmann O, Bergantz GW (2003) Rejuvenation of the Fish Canyon magma body: a window into the evolution of large-volume silicic magma systems. *Geology* 31(9):789–792
- Bachmann O, Bergantz GW (2004) On the origin of crystal-poor rhyolites: Extracted from batholithic crystal mushes. *J Petrol* 45:1565–1582
- Bachmann O, Bergantz GW (2008) The Magma Reservoirs That Feed Supereruptions. *Elements* 4(1):17–21
- Bachmann O, Dungan MA, Lipman PW (2002) The Fish Canyon magma body, San Juan volcanic field, Colorado: Rejuvenation and eruption of an upper-crustal batholith. *J Petrol* 43:1469–1503

- Bain AA, Jellinek AM, Wiebe RA (2013) Quantitative field constraints on the dynamics of silicic magma chamber rejuvenation and overturn. *Contrib Min Petr* 165(6):1275–1294
- Cannatelli C, Lima A, Bodnar RJ, De Vivo B, Webster JD, Fedele L (2007) Geochemistry of melt inclusions from the Fondo Riccio and Minopoli 1 eruptions at Campi Flegrei (Italy). *Chem Geol* 237:418–432
- Cooper KM, Kent AJR (2014) Rapid remobilization of magmatic crystals kept in cold storage. *Nature* 506:480–483
- Deering CD, Bachmann O, Vogel TA (2011) The Ammonia Tanks Tuff: erupting a melt-rich rhyolite cap and its remobilized crystal cumulate. *Earth Planet Sc Lett* 310:518–525
- De Siena L, Del Pezzo E, Bianco F (2010) Seismic attenuation imaging of Campi Flegrei: evidence of gas reservoirs, hydrothermal basins, and feeding systems. *J Geophys Res* 115(B9):1–18
- Di Renzo V, Arienzo I, Civetta L, D'Antonio M, Tonarini S, Di Vito MA, Orsi G (2011) The magmatic feeding system of the Campi Flegrei caldera: architecture and temporal evolution. *Chem Geol* 281(3–4):227–241
- Druitt TH, Costa F, Deloule E, Dungan M, Scaillet B (2012) Decadal to monthly timescales of magma transfer and reservoir growth at a caldera volcano. *Nature* 482(7383):77–80
- Elders WA, Friðleifsson GÓ, Zierenberg RA, Pope EC, Mortensen AK, Guðmundsson Á, Lowenstern JB, Marks NE, Owens L, Bird DK, Reed M (2011) Origin of a rhyolite that intruded a geothermal well while drilling at the Krafla volcano Iceland. *Geology* 39(3):231–234
- Fourmentraux C, Metrich N, Bertagnini A, Rosi M (2012) Crystal fractionation, magma step ascent, and syn-eruptive mingling: the Averno 2 eruption (Phlegrean Fields, Italy). *Contrib Min Petr* 163(6):1121–1137
- Giordano D, Russell JK, Dingwell DB (2008) Viscosity of magmatic liquids: a model. *Earth Planet Sci Lett* 271:123–143
- Girard G, Stix J (2009) Magma recharge and crystal mush rejuvenation associated with early post-collapse Upper Basin Member rhyolites, Yellowstone caldera. *Wyoming. J Petrol* 50(11):2095–2125
- Guðmundsson A (2006) How local stresses control magma-chamber ruptures, dyke injections, and eruptions in composite volcanoes. *Earth Sci Rev* 79:1–31
- Hildreth WS (2004) Volcanological perspectives on Long Valley, Mammoth Mountain, and Mono Craters: several contiguous but discrete systems. *J Vol Geoth Res* 136:169–198
- Huber C, Bachmann O, Manga M (2009) Homogenization processes in silicic magma chambers by stirring and mushification (latent heat buffering). *Earth Planet Sci Lett* 283:38–47
- Huber C, Bachmann O, Dufek J (2012) Crystal-poor versus crystal-rich ignimbrites: a competition between stirring and reactivation. *Geology* 40:115–118
- Koyaguchi T, Kaneko K (1999) A two-stage thermal evolution model of magmas in continental crust. *J Petrol* 40:241–254
- La Felice S, Landi P (2011) The 2009 paroxysmal explosions at Stromboli (Italy): magma mixing and eruption dynamics. *Bull Volc* 73(9):1147–1154
- Longo A, Barsanti M, Cassioli A, Papale P (2012a) A finite element Galerkin/least-squares method for computation of multicomponent compressible incompressible flows. *Comp Fluids* 67:57–71
- Longo A, Papale P, Vassalli M, Saccorotti G, Montagna CP, Cassioli A, Giudice S, Boschi E (2012b) Magma convection and mixing dynamics as a source of Ultra-Long-Period oscillations. *Bull Volcanol* 74:873–880
- Mangiaccapra A, Moretti R, Rutherford MJ, Civetta L, Orsi G, Papale P (2008) The deep magmatic system of the Campi Flegrei caldera (Italy). *Geophys Res Lett* 35
- Marsh BD (1981) On the crystallinity, probability of occurrence, and rheology of lava and magma. *Contrib Min Petr* 78:85–98
- Mollo S, Masotta M, Forni F, Bachmann O, De Astis G, Moore G, Scarlato P (2015) A K-feldspar-liquid hygrometer specific to alkaline differentiated magmas. *Chem Geol* 392:1–8
- Montagna CP, Papale P, Longo A (2015) Timescales of mingling in shallow magmatic reservoir. In: Caricchi L, Blundy J D (eds) *Chemical, physical and temporal evolution of volcanic systems*. Geological Society, London, Special Publications 422
- O'Brien GS, Bean CJ (2004) A 3D discrete elastic lattice method for seismic wave propagation in heterogeneous media with topography. *Geophys Res Lett* 31, L14608
- Papale P, Moretti R, Barbato D (2006) The compositional dependence of the multicomponent volatile saturation surface in silicate melts. *Chem Geol* 229:78–95
- Pappalardo L, Ottolini L, Mastrolorenzo G (2007) The Campanian Ignimbrite (southern Italy) geochemical zoning: insight on the generation of a super-eruption from catastrophic differentiation and fast withdrawal. *Contrib Min Petr* 156:1–26
- Perugini D, Poli G, Petrelli M, Campos CP, Dingwell DB (2010) Time-scales of recent Phlegrean Fields eruptions inferred from the application of a diffusive fractionation model of trace elements. *Bull Volcanol* 72(4):431–447
- Petrelli M, Perugini D, Poli G (2011) Transition to chaos and implications for time-scales of magma hybridization during mixing processes in magma chambers. *Lithos* 125(1–2):211–220
- Sacks IS, Selwyn S, Everson DW (1971) Sacks-Everson strainmeter, its installation in Japan and some preliminary results concerning strain steps. *P Jpn Acad* 47(9):707–712

- Signorelli S, Vaggelli G, Carroll C, Romano MR (2001) Volatile element zonation in Campanian Ignimbrite magmas (Phlegrean Fields, Italy): evidence from the study of glass inclusions and matrix glasses. *Contrib Min Petr* 140:543–553
- Sliwinski JT, Bachmann O, Ellis BS, Dávila-Harris P, Nelson BK, Dufek J (2015) Eruption of shallow crystal cumulates during caldera-forming events on Tenerife, Canary Islands. *J Petrol* 56(11):2173–2194
- Sparks R, Sigurdsson H, Wilson L (1977) Magma mixing: a mechanism for triggering acid explosive eruptions. *Nature* 267:315–318
- Till CB, Vazquez JA, Boyce JW (2015) Months between rejuvenation and volcanic eruption at Yellowstone caldera, Wyoming. *Geology* 43(8):695–698
- Viccaro M, Ferlito C, Cortesogno L, Cristofolini R, Gaggero L (2006) Magma mixing during the 2001 event at Mount Etna (Italy): Effects on the eruptive dynamics. *J Vol Geo Res* 149(1–2):139–159
- Voight B, Widiwijayanti C, Mattioli G S, Elsworth D, Hidayat D, Strutt M (2010) Magma-sponge hypothesis and stratovolcanoes: Case for a compressible reservoir and quasi-steady deep influx at Soufriere Hills Volcano, Montserrat. *Geophys Res Lett* 37(19): L00E05
- Wolff JA, Ellis BS, Ramos FC, Starkel WA, Boroughs S, Olin PH, Bachmann O (2015) Remelting of cumulates as a process for producing chemical zoning in silicic tuffs: A comparison of cool, wet and hot, dry rhyolitic magma systems. *Lithos* 236–237:275–286
- Zollo A, Maercklin N, Vassallo M, Dello Iacono D, Virieux J, Gasparini P (2008) Seismic reflections reveal a massive melt layer feeding Campi Flegrei caldera. *Geophys Res Lett* 35(12):L12306

Open Access This chapter is licensed under the terms of the Creative Commons Attribution 4.0 International License (<http://creativecommons.org/licenses/by/4.0/>), which permits use, sharing, adaptation, distribution and reproduction in any medium or format, as long as you give appropriate credit to the original author(s) and the source, provide a link to the Creative Commons license and indicate if changes were made.

The images or other third party material in this chapter are included in the chapter's Creative Commons license, unless indicated otherwise in a credit line to the material. If material is not included in the chapter's Creative Commons license and your intended use is not permitted by statutory regulation or exceeds the permitted use, you will need to obtain permission directly from the copyright holder.

